

# SIMULATION OF WAVE AND CURRENT FORCES ON TEMPLATE OFFSHORE STRUCTURES

Jamaloddin Noorzaei<sup>1</sup>, Samsul Imran Bahrom<sup>1\*</sup>, Mohammad Saleh Jaafar<sup>1</sup>,  
Waleed Abdul Malik Thanoon<sup>1</sup> and Shahrin Mohammad<sup>2</sup>

*Received: Feb 22, 2005; Revised: Jun 2, 2005; Accepted: Jul 11, 2005*

## Abstract

This paper describes the analytical and numerical methods adopted in developing a program for modeling wave and current forces on slender offshore structural members. Two common wave theories have been implemented in the present study, namely Airy's linear theory and Stokes' fifth order theory, based on their attractiveness for engineering use. The program is able to consider wind drift and tidal currents by simply adding the current velocity to the water velocity caused by the waves. The Morison equation was used for converting the velocity and acceleration terms into resultant forces and was extended to consider arbitrary orientations of the structural members. Furthermore, this program has been coupled to a 3-D finite element code, which can analyze any offshore structure consisting of slender members. For calibration and for comparison purposes, the developed programs were checked against a commercial software package called Structural Analysis Computer System (SACS). From the simulations of wave loading and structural analysis on few model tests, it can be concluded that the developed programs are able to reproduce results from the model tests with satisfactory accuracy.

**Keywords:** Offshore structures, wave and current forces, Airy's linear theory, Stokes' fifth order theory, Morison equation, computer program

## Introduction

It is essential for all offshore structural analysts to estimate the forces generated by fluid loading given the description of the wave and current environment (Borthwick and Herbert, 1988). In considering wave forces, the sea comprises of a large number of periodic wave components with different wave heights, periods and directions of travel which all occur at the same time in a given area. The superposition of all of these wave components coupled with their dispersive behavior leads to a randomly varying sea

surface elevation, which can be treated by statistical methods. However, to provide engineering solutions, the use of regular wave theories is common, since regular wave theories yield good mathematical models of long crested periodic waves, which are components of an irregular sea (Witz *et al.*, 1994). There is a wide range of regular wave theories ranging from the simple Airy's linear theory to the higher order formulations.

In Le Mehaute *et al.* (1968) measured water

<sup>1</sup> Civil Engineering Department, Faculty of Engineering, University Putra Malaysia, 43400, Serdang, Selangor, Malaysia, tel: +603-89466371, E-mail: jamal@eng.upm.edu.my

<sup>2</sup> Faculty of Civil Engineering, University Technology Malaysia, 81310, Johor Bahru, Malaysia

\* Corresponding author

particle velocity accuracies in percentage at the seabed, still water level, water surface as well as overall for various regular wave theories (Patel, 1989). From that study, both Airy's linear and Stokes' fifth order theory offered sufficiently good agreement for engineering use. Witz *et al.* (1994) also noted that the solution to the Stokes' fifth order theory presented by Skjelbreia and Hendrickson (1961) has been implemented widely in computer programs used within the offshore industry. Based on this, Airy's linear and Stokes' fifth order theories have been implemented in the present study.

The primary objectives of the present study is to (i) write a computer program that is able to simulate wave and current forces on template offshore structures using traditional numerical methods with minimal sacrifice towards accuracy. (ii) To couple the written program to an existing 3-D finite element program. Finally, to show the applicability of the coupled program by analyzing a simple offshore structure.

## Wave Theories

It is necessary to define the coordinate system and the terminology that will be used in the development of the wave theories in this paper. Figure 1 shows the coordinate system with  $x$  measured in the direction of the wave propagation,  $y$  measured upwards from the ground surface and  $z$  orthogonal to  $x$  and  $y$ . It is assumed that the waves are two dimensional in the  $x$ - $y$  plane and that they propagate over a smooth horizontal bed in water of constant undisturbed path. Here the following definitions hold:

SWL	=	still water level
$d$	=	distance from the seabed to the SWL
$h$	=	instantaneous vertical displacement of the sea surface above the SWL
$H$	=	height of a wave
$L$	=	wavelength (usually unknown)
$T$	=	wave period (usually known)
$c$	=	speed of wave propagation (phase speed, phase velocity, celerity, $= L/T = \omega/k$ )
$k$	=	wavenumber ( $= 2\pi/L$ )
$f$	=	wave frequency ( $= 1/T$ )
$\omega$	=	wave angular frequency ( $= 2\pi/T = 2\pi f$ )

## Formulation of Airy's Linear Theory

A relatively simple theory of wave motion, known as Airy's linear theory, was given by G.B. Airy in 1842 (Dawson, 1983). This description assumes a sinusoidal wave form whose height is small in comparison with the wavelength and the water depth. Although not strictly applicable to typical design waves used in offshore structural engineering, this theory is valuable for preliminary calculations and for revealing the basic characteristics of wave-induced water motion (Dawson, 1983).

Airy's linear theory provides an expression for horizontal and vertical water particle velocity at place  $(x, y)$  and time,  $t$  as (Dawson, 1983):

$$u = \frac{\omega H}{2} \frac{\cosh ky}{\sinh kd} \cos(kx - \omega t) \quad (1)$$

$$v = \frac{\omega H}{2} \frac{\sinh ky}{\sinh kd} \sin(kx - \omega t) \quad (2)$$

The wavenumber,  $k$  and wave angular frequency,  $\omega$  are related through the Airy's linear theory by the dispersion equation:

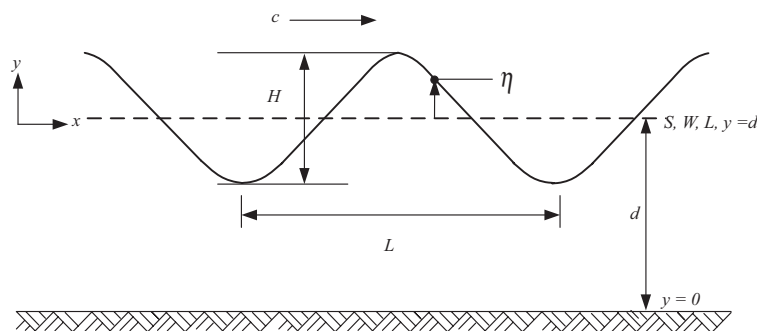


Figure 1. Definition sketch for progressive waves

$$\omega^2 = gk \tanh kd \tag{3}$$

Using the dispersion equation above, the wave speed may be expressed as:

$$c = \left(\frac{g}{k} \tanh kd\right)^{1/2} \tag{4}$$

The water particle accelerations are obtained as:  $a_x \approx du / dt$  and  $a_y \approx dv / dt$ , so that in using Eqns. (1) and (2):

$$a_x = \frac{\omega^2 H}{2} \frac{\cosh ky}{\sinh kd} \sin(kx - \omega t) \tag{5}$$

$$a_y = \frac{\omega^2 H}{2} \frac{\sinh ky}{\sinh kd} \cos(kx - \omega t) \tag{6}$$

The inherent assumption in the derivation of Airy's linear theory has a limit of  $y = d$ , which does not allow computation above the SWL (i.e.  $y > d$ ). This predicament is resolved by the linear surface correction,  $\eta$  (Charkrabarti, 1990):

$$\eta = \frac{H}{2} \cos(kx - \omega t) \tag{7}$$

Thus, at the free water surface, the vertical position of the wave becomes:

$$y = \eta + d \tag{8}$$

### Formulation of Stokes' Fifth Order Theory

Stokes' fifth order theory is derived by substituting Taylor series approximations for the variables in the free surface boundary conditions; the order of solution depends on the number of Taylor series terms included (Williams *et al.*, 1998). The method of solution for the Stokes' fifth order theory adopted in this paper is based on the methods suggested by Skjelbreia and Hendrickson (1961). Most of the algebraic complexities in their solution are in the coefficients, A denoting wave velocity parameters, B denoting wave-profile parameters and C denoting frequency parameters. These coefficients are given in explicit form by Skjelbreia and Hendrickson (1961).

The instantaneous vertical displacement of sea surface above the SWL according to Stokes' fifth order theory is described as (Dawson, 1983):

$$\eta = \frac{1}{k} \sum_{n=1}^5 F_n \cos n(kx - \omega t) \tag{9}$$

where the coefficients,  $F_n$  are given in terms of  $\lambda$  and  $B$  (refer Appendix).  $\lambda$  denotes a wave-height parameter.

For a design wave,  $\lambda$  and  $k$  are to be determined by virtue of the following pair of equations (Sarpkaya and Isaacson, 1981):

$$\frac{1}{kd} \left[ \lambda + \lambda^3 B_{33} + \lambda^5 (B_{35} + B_{55}) \right] = \frac{H}{2d} \tag{10}$$

and

$$kd \tanh(kd) \left[ 1 + \lambda^2 C_1 + \lambda^4 C_2 \right] = 4\pi^2 \frac{d}{gT^2} \tag{11}$$

Bhattacharya (1991) describes a solution to the above equations using the Newton Rhapsion method. Once the values of  $k$  and  $\lambda$  are found, the solution will then be complete and the remaining variables of interest may readily be evaluated.

The horizontal water velocity and the vertical water velocity are expressible as:

$$u = \frac{\omega}{k} \sum_{n=1}^5 G_n \frac{\cosh nky}{\sinh nkd} \cos n(kx - \omega t) \tag{12}$$

$$v = \frac{\omega}{k} \sum_{n=1}^5 G_n \frac{\sinh nky}{\sinh nkd} \sin n(kx - \omega t) \tag{13}$$

where the coefficients,  $G_n$  are functions of  $A$  (refer Appendix).

In addition to the previous relations, it is also necessary to have the frequency relation connecting the wave angular frequency,  $\omega$  with the wavenumber,  $k$ . This relation is given by the equation (Dawson, 1983):

$$\omega^2 = gk(1 + a^2C_1 + a^4C_2)\tanh kd \quad (14)$$

The wave speed is determined as in Airy's linear theory from the relation  $c = \omega/k$ , which for the Stokes' fifth order theory is expressible as:

$$c = \left[ \frac{g}{k} (1 + a^2C_1 + a^4C_2) \tanh kd \right]^{1/2} \quad (15)$$

The horizontal acceleration and vertical acceleration of the water particles can be determined respectively from the equations:

$$a_x = \frac{\partial u}{\partial t} + u \frac{\partial u}{\partial x} + v \frac{\partial u}{\partial y} \quad (16)$$

$$a_y = \frac{\partial v}{\partial t} + u \frac{\partial v}{\partial x} + v \frac{\partial v}{\partial y} \quad (17)$$

or can be written in the following explicit forms

$$a_x = \frac{kc^2}{2} \sum_{n=1}^5 R_n \sin n(kx - \omega t) \quad (18)$$

$$a_y = \frac{-kc^2}{2} \sum_{n=1}^5 S_n \cos n(kx - \omega t) \quad (19)$$

where the coefficients,  $R_n$  and  $S_n$  are given in terms of  $U_n$  and  $V_n$  (refer Appendix) :

$$U_n = G_n \frac{\cosh nky}{\sinh nkd} \quad (20)$$

$$V_n = G_n \frac{\sinh nky}{\sinh nkd} \quad (21)$$

### Determination of Wave Forces

For slender offshore structures such as monopiles, tripods or template offshore structures, the Morison equation is used for converting the velocity and acceleration terms into wave forces (Henderson *et al.*, 2003). The Morison equation may be expressed as:

$$f = \frac{1}{2} \rho C_D D |u|u + \rho C_I \frac{\pi D^2}{4} a_x \quad (22)$$

Where  $\rho$  denotes water density,  $C_D$  and  $C_I$  denote the drag and inertia coefficients respectively and  $D$  is the diameter of the member. The first term on the right hand side of this equation is referred to as the drag term and is proportional to the square of the water velocity. The second term is referred as the inertia term and is proportional to the water acceleration.

The most important consideration in applying Morison's equation is the selection of appropriate drag and inertia coefficients. However, there is considerable uncertainty in the  $C_D$  and  $C_I$  values appropriate for the calculation of offshore structural members, with many values in publication. Cassidy (1999) reviewed some published studies in the literature. He found that  $C_D$  ranged from 0.6 for smooth cylinders to 1.2 for rough cylinders.  $C_I$  ranged from 1.75 for rough cylinders to 2.0 for smooth cylinders.

The values of  $u$  and  $a_x$  in the Morison equation are calculated from an appropriate wave theory, together with chosen values of  $C_D$  and  $C_I$ . Eqn. (22) yields at any instant in the wave cycle, the force distribution along the member.

### Wave Forces on Arbitrarily Oriented Cylinders

The direction of wave force normal to the cylinder may conveniently be resolved into horizontal and vertical components. To illustrate, consider a fixed cylinder arbitrarily inclined to axes  $x$ ,  $y$  and  $z$  as shown in Figure 2.

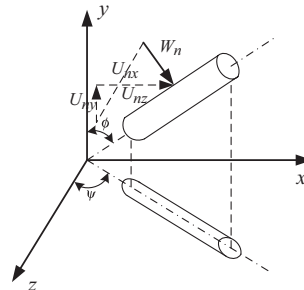


Figure 2. Definition sketch for an inclined cylinder (After Sarpkaya and Isaacson, 1981)

With polar coordinates  $\phi$  and  $\psi$  defining the orientation of the cylinder axis, the magnitude,  $|W_n|$  of the water velocity normal to the cylinder axis is given by:

$$|W_n| = [u^2 + v^2 - (c_x u + c_y v)^2]^{1/2} \quad (23)$$

and its components in the  $x$ ,  $y$ , and  $z$  directions are given respectively by:

$$\begin{aligned} U_{nx} &= u - c_x(c_x u + c_y v) \\ U_{ny} &= v - c_y(c_x u + c_y v) \\ U_{nz} &= -c_z(c_x u + c_y v) \end{aligned} \quad (24)$$

where,

$$\begin{aligned} c_x &= \sin\phi \cos\psi, \quad c_y = \cos\phi, \\ c_z &= \sin\phi \sin\psi \end{aligned} \quad (25a:b:c)$$

The components of the water acceleration in the  $x$ ,  $y$ , and  $z$  directions are given, respectively by:

$$\begin{aligned} a_{nx} &= a_x - c_x(c_x a_x + c_y a_y) \\ a_{ny} &= a_y - c_y(c_x a_x + c_y a_y) \\ a_{nz} &= c_z(c_x a_x + c_y a_y) \end{aligned} \quad (26)$$

With these relations, the components of the force per unit of cylinder length acting in the  $x$ ,  $y$ , and  $z$  directions are given respectively by the generalized Morison equations:

$$\begin{Bmatrix} f_x \\ f_y \\ f_z \end{Bmatrix} = 0.5\rho C_D D |W_n| \begin{Bmatrix} U_{nx} \\ U_{ny} \\ U_{nz} \end{Bmatrix} + 0.25\pi\rho C_1 D \begin{Bmatrix} a_{nx} \\ a_{ny} \\ a_{nz} \end{Bmatrix} \quad (27)$$

A typical offshore structural beam element may be subjected to non-uniformly distributed loading along its length arising from the above equation. These can readily be translated into forces at the beam fixed end using equilibrium equations (Witz *et al.*, 1994).

The total forces are calculated by numerical integration of the relations:

$$\begin{aligned} F_x &= \int_s f_x ds, \quad F_y = \int_s f_y ds, \\ F_z &= \int_s f_z ds \end{aligned} \quad (28a:b:c)$$

where  $s$  denotes the distance along the member axis, and the limits on the integrals are chosen to include all of the member on which the wave force acts.

### Current Velocity

The most common currents considered in offshore structural analysis are tidal currents and wind drift currents (Dawson, 1983). Both of these currents are usually regarded as horizontal and varying with depth.

The tidal current velocity profile at any vertical distance from the seabed may be determined as (Dawson, 1983):

$$U_T(y) = U_{oT} \left(\frac{y}{d}\right)^{1/7} \quad (29)$$

and, the wind drift current velocity profile may be determined as:

$$U_w(y) = U_{ow} \left(\frac{y}{d}\right) \quad (30)$$

where,  $d$  denotes the water depth,  $y$  is the vertical distance from the seabed,  $U_{oT}$  and  $U_{ow}$  denote the tidal and wind drift current velocity at the water surface respectively.

For regular design waves and a horizontal current of arbitrary depth variation, the force exerted on an offshore structure is normally calculated by simply adding the horizontal water velocity caused by the waves to that component of current velocity (Dawson, 1983).

### Verification of the Computer Program

In previous articles, brief discussion on the theoretical aspect and simulation of the wave forces on offshore structural members has been presented. A computer program written in the FORTRAN language working under the Microsoft Power Station environment has been written. The program has been validated with a standard commercial package called Structural

Analysis Computer System (SACS, version 5.1, 2001).

SACS represent wave loads that have a curved or non-linear distribution by a series of linear varying load segments using a curve fitting technique. Velocity and acceleration values are calculated for each end of the member and a linear variation is assumed between the ends. The velocity and acceleration values at the member center are calculated and compared to the values predicted by the linear variation. If either is more than 5% different from the linear distribution, then the member is segmented to include the centre point of the member. The member would now have two linear load segments. This is repeated until the 5% criterion is met. The user also has the option to set the number of equal segments desired. However, the SACS program is limited to a maximum of 10 segments (SACS Users Manual, 2001).

In the present study, the total forces are also calculated with linear segments, but without the curve fitting technique. Valuable programming time could be saved if the error committed by using a fixed number of segments compared to auto segmentation is small. Nevertheless, the present study it is not limited to 10 segments. We are to see the effects of the different number of segments with respect to the results of SACS auto segmentation. Figure 3(a) shows a discreteness of load segments of the present study for ten segments while Figure

3(b) shows a possible discreteness of load segments on a member by SACS for ten segments.

The written wave simulation program has been attached to a 3-D finite element program and the new version of the coupled finite element program is validated by analyzing a simple offshore structure by comparing the results obtained by the present study to the SACS commercial program.

### Numerical Examples

For the purposes of calibration and comparison, three numerical examples have been selected, namely:

- Numerical Example I - (comparing the results of total forces of the present study to that of SACS for a vertical cylinder).
- Numerical Example II - (comparing the results of total forces of the present study to that of SACS for an inclined cylinder).
- Numerical Example III - (structural analysis of a simple offshore structure).

Numerical Example I and II were tested under the following cases:

- Case I - Airy's linear theory
- Case II - Stokes' fifth order theory

### Numerical Example I - Problem Definition

In this example, the cylinder is considered to be in the vertical position. Initially for Case I, the forces arising from Airy's linear theory would

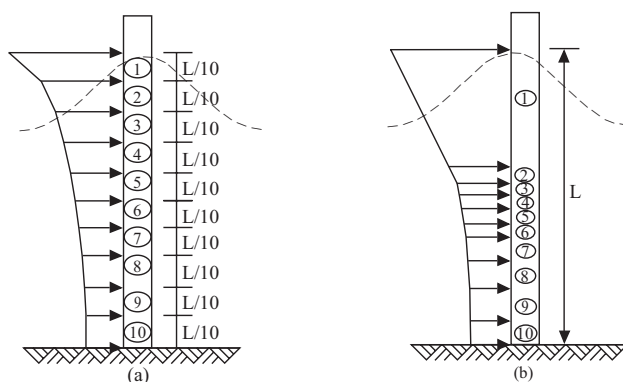


**Figure 3. (a) Discreteness of the present study for ten segments  
(b) A possible discreteness on a member by SACS for ten segments**

be calculated and subsequently for Case II, the forces arising from Stokes' fifth order theory would be calculated. In each Case, the distributed wave force acting on the cylinder arising from the present study would be divided into 5, 10 and 15 segments respectively to calibrate and compare which number of segments would correspond closest to the results of the SACS program. The wave parameters and cylinder details used in Numerical Example I are presented in Figure 4. The values of  $C_D$  and  $C_I$  are based from Dawson (1983).

## Results and Discussion on Numerical Example I

### Case I

Figure 5 shows the distribution of wave forces plus currents for a vertical cylinder arising from Airy's linear theory for different values of phase angle. The data in that figure show that all results of the present study slightly underestimated the results of the SACS program. The average percentage error of the present study compared to SACS is 1.68%, 2.62%, and 2.80% for 5, 10, and 15 segments respectively. The slight disagreement between the present study to that of SACS may lie in the tolerance for the iteration of Egn. (3) to obtain the wavenumber,  $k$ . In the present study, the tolerance was set to 5 decimal places. From Table 1, we can see a slight difference for the wavenumber value obtained

from the present study to that of SACS. The wavenumber is used in most equations of the wave kinematics, thus affecting subsequent results. Another evident reason for the disagreements is of course, the auto segmentation of the SACS program. The free water surface profile predicted by present study to that of SACS are plotted in Figure 6. It is seen from these plots, both programs gave identical results.

As mentioned earlier, Airy's linear theory is not generally valid for deep water, thus the estimated error in using this theory over the more accurate theories can be made by utilizing Figure 7 (Dawson, 1983). It is obvious from this figure that the ratio of water depth to wavelength for this case is approximately 2.0. But the ratio of water depth to wavelength of 0.2 occurs at a value of the ratio of wave height to wavelength of 0.04. This corresponds to a 10% error. For the design wave in this example, the ratio of wave height to wavelength is 0.09, thus the estimated error in using Airy's linear theory is approximately  $10 \times 0.09 / 0.04 = 22\%$ .

### Case II

Figure 8 shows the distribution of wave forces plus currents for a vertical cylinder arising from Stokes' fifth order theory for different phase angles. A similar trend can be seen to that of the results of the previous case, with all results of the present study slightly underestimating the results of the SACS

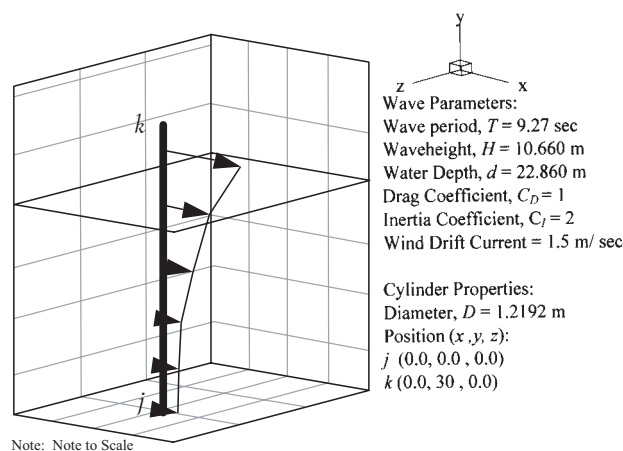


Figure 4. Definition sketch for numerical example I

program. The average percentage difference of the present study compared to SACS is 1.96%, 2.62%, and 2.74%, for 5, 10, and 15 segments respectively.

Figure 9 shows the surface elevation arising from the Stokes' fifth order theory for different phase angles. It can be seen that the results of SACS and the present study have good agreement in modeling the free water surface. Table 2 shows the wavenumber and wavelength predicted by SACS and the present study arising from Stokes' fifth order theory. From that table, it is seen that the present study underestimated the wavelength by 0.64 m. This may be due to the techniques employed in solving Eqns. 10 and 11.

Even with the same wave parameters as in Case I, it is clear that in this Case, wave loads predicted from Stokes' fifth order theory are significantly higher compared to that of Airy's linear theory. From Figures 5 and 8 the maximum horizontal force arising from Airy's linear theory predicted by SACS is 357.46 KN and the maximum horizontal force arising from Stokes' fifth order theory predicted by SACS is 444.35 KN respectively. In this Case, Airy's linear theory underestimated the forces arising from Stokes' fifth order theory by 19.6%, which very close to the estimated error discussed in Case I.

Among the reasons why Stokes' fifth order theory predicts larger values of forces in this case are: (i) Stokes' fifth order theory models the free water surface more accurately producing steeper crests and lower troughs as illustrated in Figure 9. In this Case, the crests obtained using Stokes' fifth order theory increased by about 1.52 m and the trough increased by about 1.49 m compared to Airy's linear theory. (ii) Stokes' fifth order theory retains the convective accelerations terms (Eqns. 16 and 17) whereas Airy's linear theory neglects them.

## Numerical Example II - Problem Definition

In this example, the validation procedures, assumptions and wave parameters made are similar to Numerical Example I, the exception being that in this case, the cylinder is considered to be in an arbitrarily oriented position. It is important to test the cylinder in an arbitrarily oriented position as to consider the forces in the  $y$  and  $z$  directions and the geometrical effect of the oriented member towards the free water surface profile. A definition sketch for Numerical Example II is illustrated in Figure 10.

**Table 1. Wavenumber and wavelength predicted by SACS and the present study arising from Airy's linear theory**

Program	Wavenumber	Wavelength (m)
Present study	0.05503	114.168
SACS	0.05506	114.105

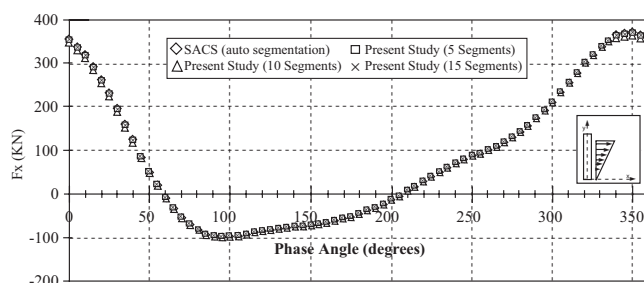


**Figure 5. Distribution of wave forces plus currents for a vertical cylinder arising from Airy's linear theory**

**Results and Discussion on Numerical Example-II**

**Case I**

Figure 11(a) shows the distribution of wave forces plus currents for an inclined cylinder arising from Airy's linear theory for different phase angles in the *x*-direction. For forces in the *x*-direction, there is a good agreement between the distributions of the forces predicted by both programs, however in the phase angle between 235 and 250 degrees there is a slight deviation between the two programs. Due to the scale chosen, these values are not apparent in Figure 11(a). This figure is magnified in Figure 12 to illustrate errors obtained in this Case. In this figure for example, the force obtained by SACS at the phase angle of 235 degrees is -1.17 KN, and at the same phase angle, the present study (for 5 segments) obtained a value of -2.84 KN.

The distributions of forces in the *y* and *z* directions for different phase angles are

illustrated in Figures 11(b-c) respectively. It is clear from these plots, that there is a good agreement between the forces evaluated from the present study to that of SACS.

The surface elevation with respect to the orientation of the member obtained by the present study is presented in Figure 13. It can be seen that because the member is arbitrarily oriented, the crest is produced later compared to the vertical condition. The crest of the water surface for the oriented member in this Case occurs at approximately 15.32 m from the origin.

**Case II**

Figures 14(a-c) show the distribution of wave forces plus currents for an inclined cylinder arising from Stokes' fifth order theory for different phase angles in the *x*, *y* and *z* directions respectively. It is obvious from these plots that there is a good comparison between the results

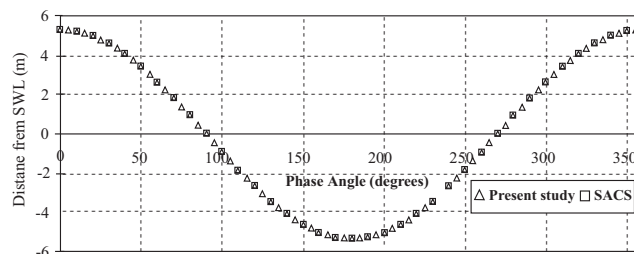


**Figure 6. Surface elevation arising from Airy's linear theory at different phase angles**

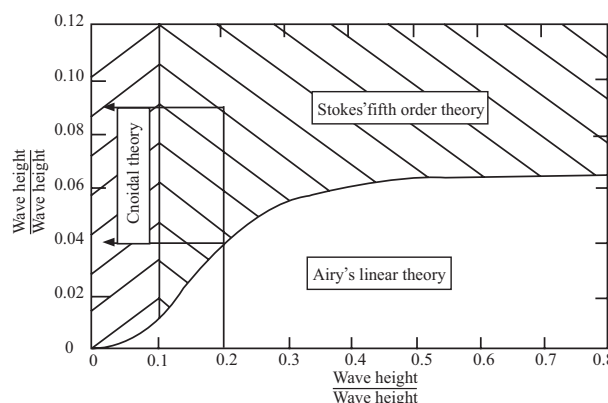


**Figure 7. Diagram showing the range of validity of Airy's linear theory, assuming tolerable errors of no more than 10%**

predicted by both programs. However, Figure 14(c) indicates that there is a marginal difference for the forces between the phase angle of 300 and 360 degrees. This could be due to the large number and complex nature of the coefficients for higher order solutions, thus small algebraic errors can occur. Results reported by different analysts tend to vary as reported in the literature by Barltrop and Adams (1991).

Figure 15 compares the surface elevation for the previous vertical position of the member (Numerical example I, Case II) to the present inclined position. The distance from origin where the crest occurs for this case was evaluated approximately 16.08 m from the origin.

### Numerical Example III - Problem Definition

The accuracy of the simulation program to calculate wave and current forces has been presented in the previous two examples. In the next phase of this investigation, this program is coupled to an existing 3-D general purpose finite element code. The

verification of the coupled program is shown by analyzing a simple offshore structure. The formulations of the finite element program is beyond this paper, however conventional beam elements have been used that closely follows the formulation presented Figure 16 shows the 3-D finite element idealization of a simple offshore structure (Dawson, 1983) used in this example, with the wave propagating in the  $x$ -direction.

### Results for Numerical Example III

The position of the wave crest in relation to the structure is an important parameter, which must be inputted into the computer program. The wave crest should be located such that the maximum possible shear and moments are applied to the structure (McClelland and Reifel, 1986). Figures 17 and 18 shows the phase angle that causes the maximum horizontal force (resulting in maximum shear) arising from Airy's linear and Stokes' fifth order theory respectively. From these two figures, the total horizontal force arising from Airy's linear theory and Stokes' fifth order theory are

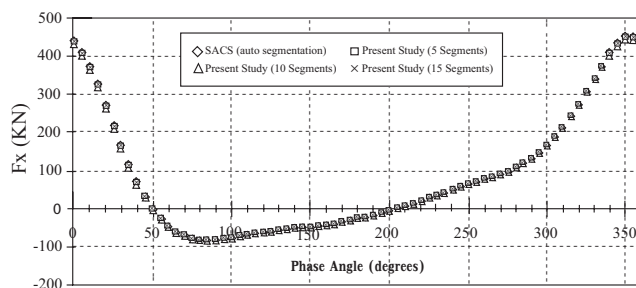


Figure 8. Distribution of wave forces plus currents for a vertical cylinder arising from Stokes' fifth order theory

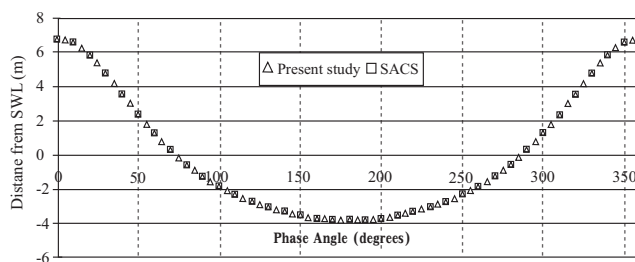


Figure 9. Surface elevation arising from Stokes' fifth order theory at different phase angles

almost identical. The phase angle that causes the maximum horizontal force coincidentally occurs at a phase angle of 0 and 360 degrees. Thus, any one of these values may be inputted in the program since 0 degrees and 360 degrees are actually the same position in a wave cycle.

Figure 19 shows the displacements along leg A for forces arising from Airy's linear theory. From Figure 19, the present study obtained smaller values with respect to SACS auto segmentation with a percentage difference for node 3 of 5.43%, 5.71%, and 5.76%, for 5, 10, and 15 segments respectively. It can be stated that as number of segments are increasing due to the load redistribution, the resulting displacements are converging. However, an attempt has been made to divide the load distribution into 10 equal segments for both programs in order to have a clear comparison between them. Thus, the displacements due to SACS set for 10 equal segments are also exhibited in Figure 19. In this case, the percentage difference between SACS set for 10 equal segments to the present study set for 10 equal segments is only 1.56%.

Figure 20 shows the displacements along leg A for forces arising from Stokes' fifth order theory. From Figure 20, the present study obtained smaller values with respect to SACS auto segmentation with a percentage difference for node 3 of 6.1%, 6.41%, and 6.46% for 5, 10, and 15 segments respectively. The percentage difference between SACS set for 10 equal segments to the present study set for 10 equal segments in this case is 2.30%.

It is established that SACS tend to produce larger values compared to the present study when the auto segmentation option is used. The deflected profile for the entire offshore structure obtained from the present study is illustrated in Figure 21.

The comparison of member end forces and moments for selective elements obtained through the present study and SACS (using Airy's linear theory and Stokes' fifth order theory) are tabulated in Tables 3 through 6 respectively. It is clear from these tables, that the coupled program is able to reproduce results with respect to SACS with good accuracy.

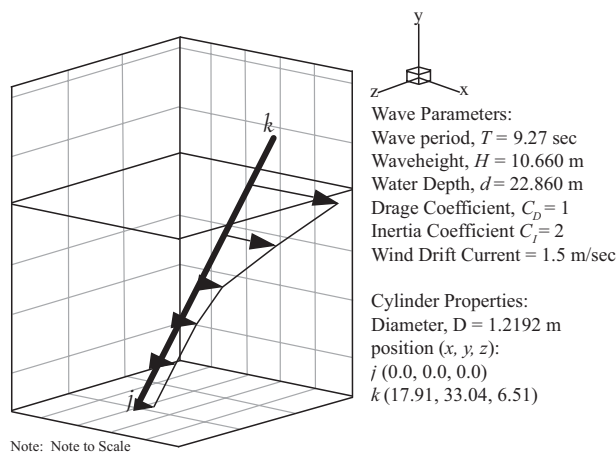


Figure 10. Definition sketch for numerical example II

Table 2. Wavenumber and wavelength predicted by SACS and the present study arising from Stokes' fifth order theory

Program	Wavenumber	Wavelength (m)
Present study	0.05067	124.002
SACS	0.05039	124.692

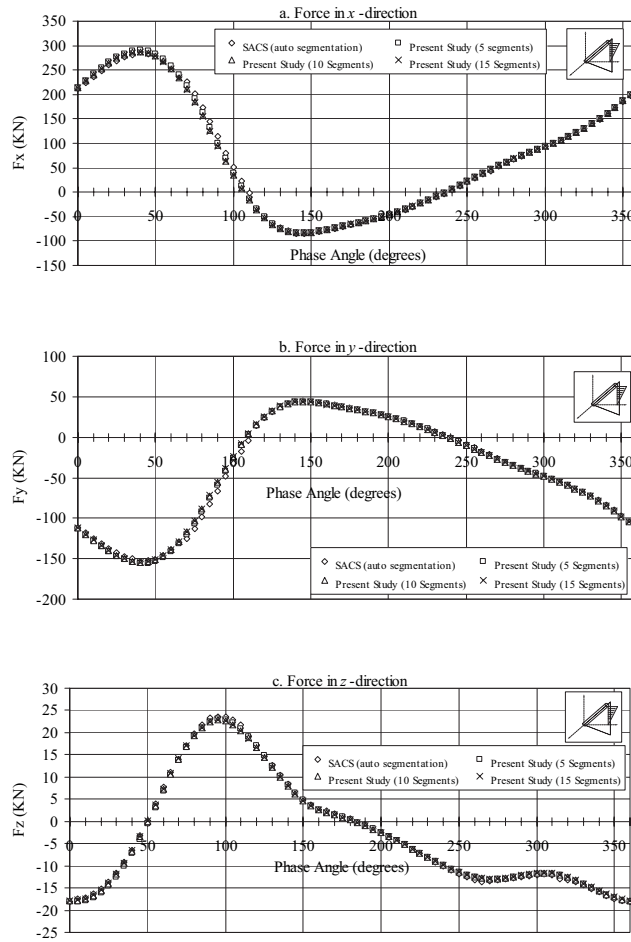


Figure 11. Comparison of the distribution of wave forces plus currents obtained from the present study and SACS arising from Airy's linear theory at different phase angles in x, y and z directions respectively

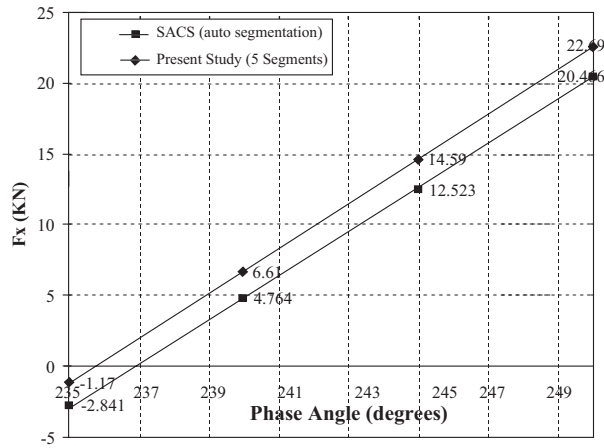


Figure 12. Magnification of Figure 11(a) for phase angle between 235 and 250 degrees

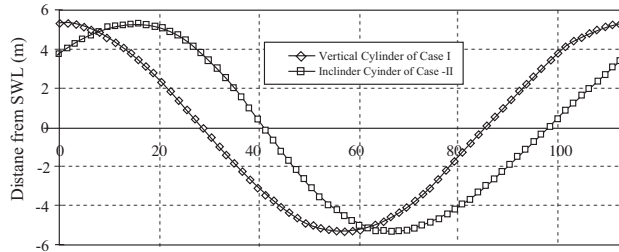


Figure 13. Comparison of the surface elevation arising from Airy's linear theory for a vertical and inclined member

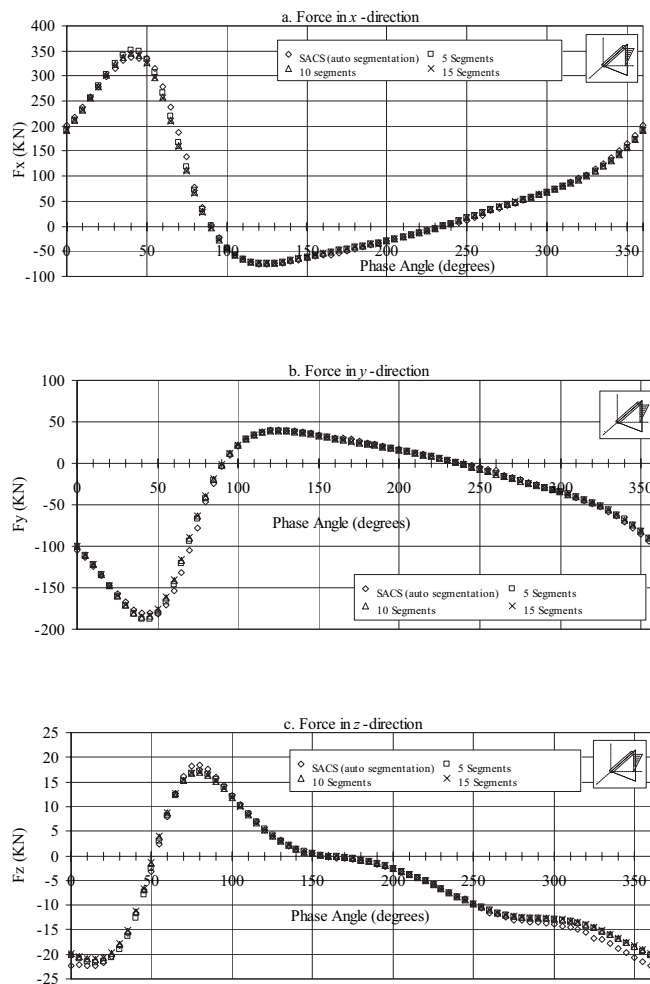


Figure 14. Comparison of the distribution of wave forces plus currents obtained from the present study and SACS arising from Stokes, fifth order theory at different phase angles in x, y, and z directions respectively

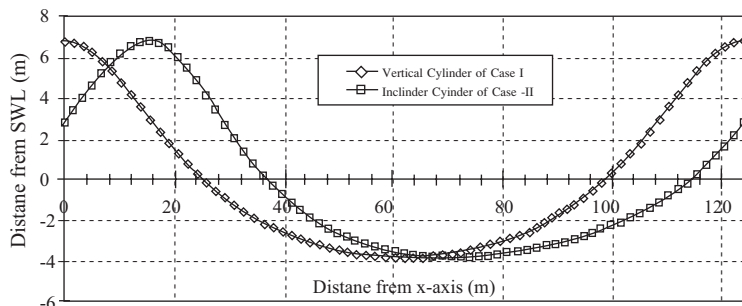


Figure 15. Comparison of surface elevation arising from Stokes, fifth order theory for a vertical and inclined member

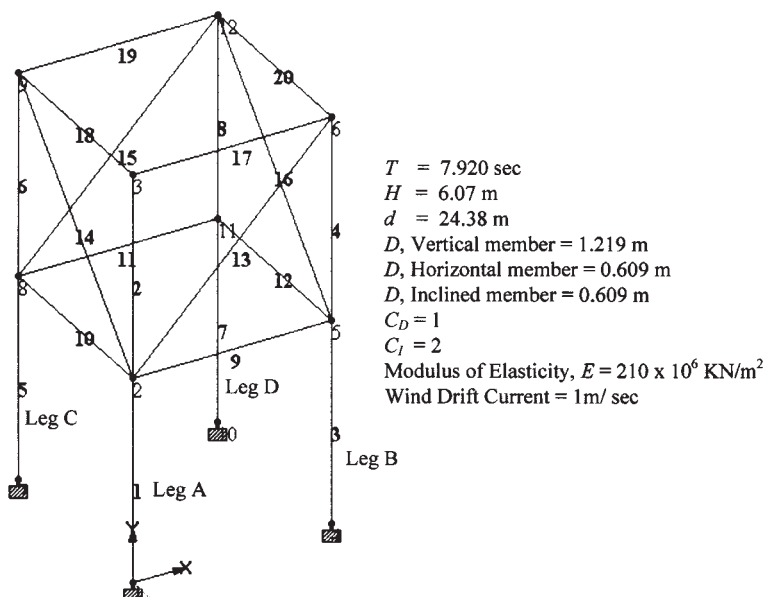


Figure 16. Offshore structure considered in numerical example III (After Dawson, 1983)

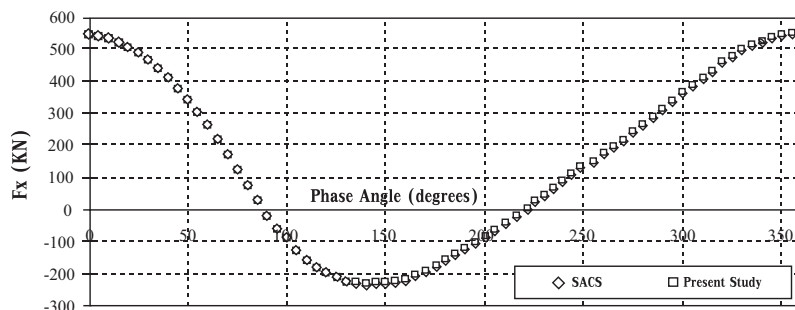


Figure 17. The phase angle resulting in maximum horizontal force arising from Airy's linear theory

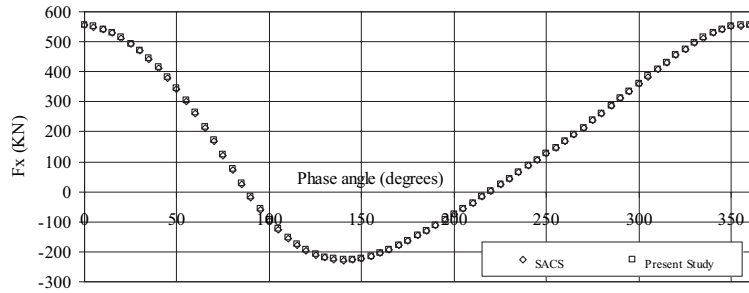


Figure 18. The phase angle resulting in maximum horizontal force arising from Stokes' fifth order theory

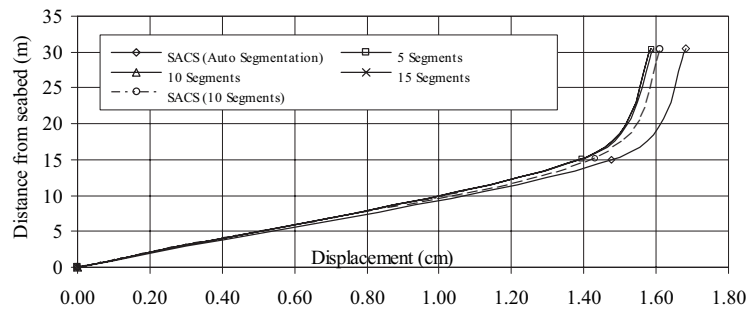


Figure 19. Comparison of displacements of the present study vs SACS resulting from Airy's linear theory

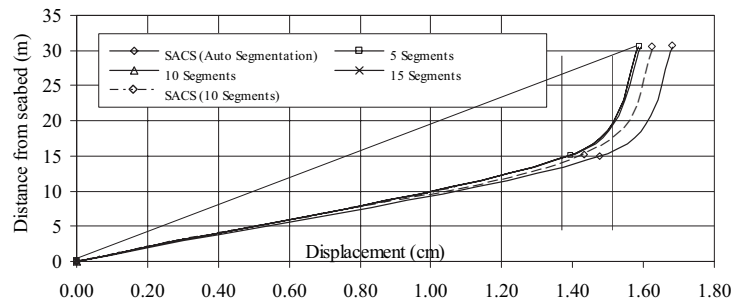


Figure 20. Comparison of displacements of the present study vs SACS resulting from Stokes, fifth order theory

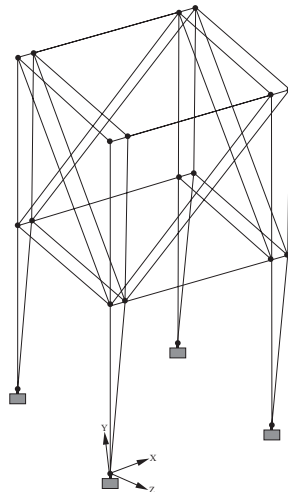


Figure 21. Deflected profile of the structure

Table 3. Comparison of member end forces for selective members obtained from SACS and the present study arising from Airy's linear theory

Member no.	Member ends	Force (KN)					
		SACS (auto segmentation)			Present study (5 segments)		
		$F_x$	$F_y$	$F_z$	$F_x$	$F_y$	$F_z$
17	3	84.15	4.01	1.24	82.22	4.01	1.24
	6	-84.15	-4.01	-1.24	-82.22	-4.01	-1.24
18	3	3.67	0.19	-0.81	3.65	0.19	-0.85
	9	-3.67	-0.19	0.81	-3.65	-0.19	0.85
19	6	99.65	4.11	-3.25	97.59	4.11	-3.16
	12	-99.65	-4.11	3.25	-97.59	-4.11	3.16
20	9	-3.17	-0.20	-0.19	-2.99	-0.18	-0.22
	12	3.17	0.20	0.19	2.99	0.18	0.22

Table 4. Comparison of member end forces for selective members obtained from SACS and the present study arising from Stokes, fifth order theory

Member no.	Member ends	Force (KN)					
		SACS (auto segmentation)			Present study (5 segments)		
		$F_x$	$F_y$	$F_z$	$F_x$	$F_y$	$F_z$
17	3	84.15	4.01	1.24	82.22	4.01	1.24
	6	-84.15	-4.01	-1.24	-82.22	-4.01	-1.24
18	3	3.67	0.19	-0.81	3.65	0.19	-0.85
	9	-3.67	-0.19	0.81	-3.65	-0.19	0.85
19	6	99.65	4.11	-3.25	97.59	4.11	-3.16
	12	-99.65	-4.11	3.25	-97.59	-4.11	3.16
20	9	-3.17	-0.20	-0.19	-2.99	-0.18	-0.22
	12	3.17	0.20	0.19	2.99	0.18	0.22

**Table 5. Comparison of member end moments for selective members obtained from SACS and the present study arising from Airy's linear theory**

Member no.	Member ends	Force (KN)					
		SACS (auto segmentation)			Present study (5 segments)		
		$F_x$	$F_y$	$F_z$	$F_x$	$F_y$	$F_z$
17	3	0.35	-10.52	30.79	0.34	-10.50	30.85
	6	-0.35	-8.36	30.29	-0.34	-8.41	30.33
18	3	0.22	-1.48	1.34	0.21	-0.90	1.36
	9	-0.22	13.75	1.60	-0.21	13.91	1.59
19	6	0.45	27.35	31.95	0.43	26.63	31.96
	12	-0.452	2.20	30.72	-0.43	21.53	30.73
20	9	-0.05	-2.53	-1.48	-0.06	-2.10	-1.41
	12	0.05	5.39	-1.50	0.06	5.52	-1.40

**Table 6. Comparison of member end moments for selective members obtained from SACS and the present study arising from Stokes' fifth order theory**

Member no.	Member ends	Force (KN)					
		SACS (auto segmentation)			Present study (5 segments)		
		$F_x$	$F_y$	$F_z$	$F_x$	$F_y$	$F_z$
17	3	0.35	-10.52	30.79	0.34	-10.50	30.85
	6	-0.35	-8.36	30.29	-0.34	-8.41	30.33
18	3	0.22	-1.48	1.34	0.21	-0.90	1.36
	9	-0.22	13.75	1.60	-0.21	13.91	1.59
19	6	0.45	27.35	31.95	0.43	26.63	31.96
	12	-0.45	22.20	30.72	-0.43	21.53	30.73
20	9	-0.05	-2.53	-1.48	-0.06	-2.10	-1.41
	12	0.05	5.39	-1.50	0.06	5.52	-1.40

## Conclusion

From the simulations of wave loading on a vertical and inclined cylinder, it can be concluded that the developed program is able to reproduce results from the model tests with satisfactory accuracy. The wave simulation program has been coupled with a 3-D finite element program and the applicability and accuracy of the coupled program has been demonstrated by analyzing a simple offshore structure. For individual members, the error committed in using Airy's linear theory for deep water is apparent, however when analyzing a whole offshore structure, the theory is able to give a good representation of the wave loads compared to the more accurate but complex

Stokes' fifth order theory. It is seen that SACS auto segmentation will give larger results compared to dividing the load distribution into equal segments. The wave characteristics produced by the present study are also in agreement with what is available in the literature.

## Acknowledgements

The authors would like to thank Mr. Shaharuddin Ismail of Malaysian Mining Corporation (MMC) oil and gas Engineering and Ir. Rafee Makbol (formerly of MMC oil and gas Engineering) for making the results of the SACS program available to the authors.

## References

- Bartrop, N.D.P., and Adams, A.J. (1991). Dynamics of fixed marine structures. 3<sup>rd</sup> ed. Butterworth-Heinemann, Oxford, UK, **number of pages**.
- Bhattacharyya, S.K. (1991). Dispersion of fifth order stokes waves: A numerical method. Technical Note, Adv. Eng. Software, Computer Mechanics Publication, 13(1):41-45.
- Borthwick, A.G.L., and Herbert, D.M. (1988). Loading and response of a small diameter flexibly mounted cylinder in waves. **Journal of Fluids and Structures**, Academic Press Limited, 2:479-501.
- Cassidy, M.J. (1999). Non-linear analysis of jack-up structures subjected to random waves, [Ph.D. thesis]. University of Oxford, **number of pages**.
- Chakrabarti, S.K. (1990). Nonlinear Methods in Offshore Engineering. Developments in Marine Technology. **boom edition**. Elsevier, London, U.K, **total number of page**.
- Dawson, T.H. (1983). Offshore Structural Engineering. **book edition**. Prentice Hall, Englewood Cliffs, N.J., USA, **total number of pages**.
- Henderson, A.R., Zaaier, M.B., and Camp, T.R. (2003). Hydrodynamic loading on offshore wind turbines. Proceedings of OWEMES Conference; inclusive date of Conf.; Naples, Italy, **number of page**.
- McClelland, B., and Reifel, M.D. (1986). Planning and Design of Fixed Offshore Platforms. **book edition**. Van Nostrand Reinhold Company, NY, USA, **number of pages**.
- Patel, M.H. (1989). Dynamics of Offshore Structures. **book edition**. Butterworths, London, UK, **total number of pages**.
- SACS Users Manual. (2001). Seastate. Release 5: Revision 4, Engineering Dynamics, Inc, USA, **total number of pages**.
- Sarpkaya, T., and Isaacson, M. (1981). Mechanics of Wave Forces on Offshore Structures. **book editon**. Van Nostrand Reinhold Company, NY, p. 323-331.
- Skjelbreia, L., and Hendrickson, J.A. (1961). Fifth order gravity wave theory. Proceedings of 7<sup>th</sup> Coastal Eng. Conf., The Hague, p. 184-196.
- Weaver, W.Jr., and Gere, M. (1986). Matrix Analysis of Framed Structures. **book editon**. Van Nostrand Reinhold Company, NY, USA, **total number of pages**.
- Williams, M.S., Thompson, R.S.G., and Houlsby, G.T. (1998). Non-linear analysis of off shore jack-up units. Computers and Structures, 69(Pergamon):171-180.
- Witz, J., Lyons, G., Patel, M.H., and Brown, D. (1994). Advanced Offshore Engineering. Offshore Engineering Handbook Series. **book edition**. Bentham Press, London, UK, **total number of pages**.

## Appendix

$$\begin{aligned}
 F_1 &= \lambda \\
 F_2 &= \lambda^2 B_{22} + \lambda^4 B_{24} \\
 F_3 &= \lambda^3 B_{33} + \lambda^5 B_{35} \\
 F_4 &= \lambda^4 B_{44} \\
 F_5 &= \lambda^5 B_{55}
 \end{aligned} \tag{A.1}$$

$$\begin{aligned}
 G_1 &= \lambda A_{11} \sin kd + \lambda^3 A_{13} \sin kd + \lambda^5 A_{15} \sin kd \\
 G_2 &= 2\lambda^2 (A_{22} \sin 2kd + \lambda^4 \sin 2kd) \\
 G_3 &= 3(\lambda^3 \sin 3kd + \lambda^5 \sin 3kd) \\
 G_4 &= 4\lambda^4 A_{44} \sin 4kd \\
 G_5 &= 5(\lambda^5 A_{55} \sin 5kd)
 \end{aligned} \tag{A.2}$$

$$\begin{aligned}
 R_1 &= 2U_1 - U_1 U_2 - V_1 V_2 - U_2 U_3 - V_2 V_3 \\
 R_2 &= 4U_2 - U_1^2 + V_1^2 - 2U_1 U_3 - 2V_1 V_3 \\
 R_3 &= 6U_3 - 3U_1 U_2 + 3V_1 V_2 - 3U_1 U_4 - 3V_1 V_4 \\
 R_4 &= 8U_4 - 2U_2^2 + 2V_2^2 - 4U_1 U_3 + 4V_1 V_3 \\
 R_5 &= 10U_5 - 5U_1 U_4 - 5U_2 U_3 + 5V_1 V_4 + 5V_2 V_3
 \end{aligned} \tag{A.3}$$

$$\begin{aligned}
 S_0 &= -2U_1 V_1 \\
 S_1 &= 2V_1 - 3U_1 V_2 - 3U_2 V_1 - 5U_2 V_3 - 5U_3 V_2 \\
 S_2 &= 4V_2 - 4U_1 V_3 - 4U_3 V_1 \\
 S_3 &= 6V_3 - U_1 V_2 + U_2 V_1 - 5U_4 V_1 - 5U_4 V_1 \\
 S_4 &= 8V_4 - 2U_1 V_3 + 2U_3 V_1 + 4U_2 V_2 \\
 S_5 &= 10V_5 - 3U_1 V_4 + 3U_4 V_1 - U_2 V_3 + U_3 V_2
 \end{aligned} \tag{A.4}$$